

DTP/94/112
 UR-1397
 ER-40685-845
 November 1994

Gluon Radiation in $t\bar{t}$ Production at the Tevatron $p\bar{p}$ Collider

Lynne H. Orr

*Department of Physics, University of Rochester
 Rochester, NY 14627-0171, USA*

T. Stelzer

*Department of Physics, University of Durham
 Durham DH1 3LE, England*

and

W.J. Stirling

*Departments of Physics and Mathematical Sciences, University of Durham
 Durham DH1 3LE, England*

Abstract

We present a complete calculation of the matrix elements for the processes $q\bar{q}, gg \rightarrow bW^+\bar{b}W^-g$ and $qg \rightarrow bW^+\bar{b}W^-q$ which are relevant for the study of events with an additional jet in $t\bar{t}$ production at the Tevatron $p\bar{p}$ collider. Our calculation includes (i) the contributions from gluons emitted during the top production and decay stages and the interference between these, and (ii) the complete set of Feynman diagrams corresponding to both resonant and non-resonant top production. We study the distribution in phase space of the additional parton jet and make comparisons with previous studies based on the soft-gluon approximation and with results from parton-shower Monte Carlo simulations. The implications for top mass measurements are briefly discussed.

1 Introduction

A significant number of top quark candidate events reported by the CDF [1] and D0 [2] collaborations at the Tevatron $p\bar{p}$ collider contain an extra hadronic jet, in addition to those expected from the leading-order processes $q\bar{q}, gg \rightarrow t\bar{t} \rightarrow b\bar{b}W^+W^-$. Such jets can be produced, for example, by gluons emitted from the incoming partons, from the top quarks before or after they decay, or from the b quarks in the final state. Events with such ‘extra’ jets are important from both the experimental and theoretical viewpoints. Experimentally, they can complicate the identification and measurement of the top quark, for example when a gluon jet is wrongly identified as a b jet. They can also, at least in principle, distort the measurement of the top mass when some of the top quark four-momentum is carried by a jet which is not identified as one of the decay products.

There have been several recent studies of extra jets in top production. In Ref. [3], a complete treatment of all the various contributions was presented in the ‘soft-gluon’ approximation. This work built on previous studies [4, 5, 6] of radiation off heavy unstable objects. In Ref. [7], the impact of hard-gluon radiation on top mass reconstruction was investigated, using a stable, on-shell top quark approximation which factorizes the gluon emission into $p\bar{p} \rightarrow t\bar{t}g$ and $t \rightarrow W^+bg$ (or $\bar{t} \rightarrow W^-\bar{b}g$) contributions. And of course the parton-shower Monte Carlo programs used in the experimental analyses naturally give rise to events with extra jets. However these are based on collinear approximations to matrix elements and, in some cases, may have certain types of gluon emission missing.

In this paper we present the first complete calculation of the exact matrix elements for the processes $q\bar{q}, gg \rightarrow bW^+\bar{b}W^-g$ and $qg \rightarrow bW^+\bar{b}W^-q$, including (i) the contributions from gluons emitted during the top production and decay stages and the interference between these, and (ii) the complete set of Feynman diagrams corresponding to both resonant and non-resonant top production. In the same way that the VECBOS [8] matrix-element-based program is successfully used to analyze $W, Z +$ jets events, we would expect our calculation to provide the most accurate predictions for those events in which an additional energetic jet in association with the usual $t\bar{t}$ decay products is observed.

The remainder of the paper is organized as follows. In the next section we describe how the matrix elements are calculated using the MadGraph program [9]. We discuss how these matrix elements are interfaced with the phase space generator to produce cross sections, and how it is possible to classify the emitted gluons as originating at either the top production or decay stages. In Section 3 we describe the set of kinematical cuts which enables us to define and calculate a $bW^+\bar{b}W^- +$ jet cross section that is relevant to the experimental measurements. We present distributions of the jet E_T and pseudorapidity, and also of the separation between the jet and the b quarks, an important quantity when attempting to reconstruct the top momentum. Some illus-

trative invariant mass distributions are also presented. In Section 4 we compare our distributions with those from the HERWIG [10] parton-shower Monte Carlo program, one of the main analysis tools used in the experimental analyses. We make a careful comparison of the jet distributions obtained in our matrix-element (ME) approach with those generated by the parton-shower (PS) approach, since any differences *could* have important implications for the measurement of the top mass. Finally, we present our conclusions in Section 5.

2 Calculation of the cross section

As mentioned in the Introduction, previous works have investigated the effects of gluon radiation beyond leading order in either the ‘stable top’ [7] or ‘soft-gluon’ approximations [3, 5, 6]. In this study we focus on $t\bar{t}$ production in association with an extra jet which is identified as such in the experiment.¹ We perform the complete $O(\alpha_s^3)$ tree-level matrix element calculation, including top width effects, radiation off the top decay products, and all interferences.

In $p\bar{p}$ collisions there are three relevant parton-level processes which may contribute to $t\bar{t}$ production with an additional jet:

1. $q\bar{q} \rightarrow b\bar{b}W^+W^-g$,
2. $gg \rightarrow b\bar{b}W^+W^-g$,
3. $g\bar{q} \rightarrow b\bar{b}W^+W^-q$.

Subprocesses one and three are related by crossing and consist of 90 Feynman diagrams, while subprocess two consists of 222 Feynman diagrams. The complete set of diagrams and the corresponding helicity-amplitude code were generated automatically using the MadGraph [9] package. In practice, the contribution from subprocess three is very small, the extra jet is almost always a gluon jet (and for simplicity will be referred to as such in what follows). Furthermore, the contribution from subprocess two (gg fusion) is suppressed by the gluon density in the proton. Therefore, although the full set of diagrams was used to generate the figures presented in this paper, a reasonable approximation can be obtained by using the 7 $q\bar{q} \rightarrow t\bar{t}$ production diagrams shown in Fig. 1.² We neglect radiation off the decay products of the W ’s; this is equivalent to assuming either that (i) the W ’s decay leptonically, or (ii) strict cuts on the mass reconstruction of the W will largely eliminate events where the W decays

¹In Ref. [7] the emphasis was on events with the leading-order number of jets, but which contain either additional radiation close to the primary jets or wide-angle radiation not identified as an extra jet.

²Note that the $q\bar{q}$ annihilation cross section is an order of magnitude larger than the gg fusion cross section for $t\bar{t}$ production with $m_t \sim 174$ GeV at the Tevatron collider.

into three well-separated jets. In practice this is a reasonable first approximation, but in principle the analysis could be extended to include the hadronic decay of one of the W bosons, and the corresponding radiation off the $q\bar{q}'$ decay products.

In Ref. [3], where the production of an extra jet was analyzed in the soft approximation, it was shown that the gluon emission could be separated unambiguously into ‘production’ and ‘decay’ contributions, together with interferences between them. The former includes emission off the incoming partons and off the top quark *before* it weak decays. The latter includes emission off the top quark *during* its decay, and off the daughter b quarks. The interference between these types of emissions is only important for soft gluons whose energy is comparable to the top width, $E_g \sim \Gamma_t$ [4, 5, 6].

In the context of our exact calculation, the separation into production and decay contributions is not completely unambiguous (nor gauge invariant in general), but a consistent operational definition based on partitioning the phase space can be formulated as follows. Production emission is defined as those regions of phase space for which the masses of the $W^- + \bar{b}$ and $W^+ + b$ systems reconstruct to the top mass. Decay emission is defined as those regions of phase space for which either the $W^- + \bar{b}$ or $W^+ + b$ system requires the inclusion of the extra jet to give the top mass. This is implemented by comparing the relative sizes of the Breit-Wigner resonances which appear in the matrix element. Explicitly, we define

$$\begin{aligned}
S_{\text{prod}} &= \left| ((p_{W^+} + p_b)^2 - m_t^2 + im_t\Gamma_t) \times ((p_{W^-} + p_{\bar{b}})^2 - m_t^2 + im_t\Gamma_t) \right| \\
S_1 &= ((p_{W^+} + p_b)^2 - m_t^2 + im_t\Gamma_t) \times ((p_{W^-} + p_{\bar{b}} + p_{\text{jet}})^2 - m_t^2 + im_t\Gamma_t) \\
S_2 &= ((p_{W^+} + p_b + p_{\text{jet}})^2 - m_t^2 + im_t\Gamma_t) \times ((p_{W^-} + p_{\bar{b}})^2 - m_t^2 + im_t\Gamma_t) \\
S_{\text{dec}} &= \min(|S_1|, |S_2|).
\end{aligned} \tag{1}$$

An event is then labeled as production emission if $S_{\text{prod}} < S_{\text{dec}}$, and as decay emission if $S_{\text{prod}} > S_{\text{dec}}$. This definition is gauge invariant and can be used in any region of phase space for any set of cuts. Since the jet E_T^{min} cut will remove the contribution from very soft gluon emission, one finds that for most events which pass the cuts either $S_{\text{prod}} \ll S_{\text{dec}}$ or $S_{\text{dec}} \ll S_{\text{prod}}$. For such events production emission is well described by diagrams 1–5 in Fig. 1, and decay emission is well described by diagrams 4–7.³ This decomposition of the radiation is the natural generalization of the definition used in Refs. [3, 5, 6] and proves useful in understanding the distribution of the radiation.

3 A study of $bW^+\bar{b}W^- + \text{jet}$ production

³Note that diagrams 4 and 5 can contribute to *both* types of emission, depending on whether the top quark (or \bar{t}) is closer to being on shell before or after it radiates the gluon.

3.1 Definition of the jet cross section

Our aim is to calculate the cross section for the production of an extra, identifiable jet in $t\bar{t}$ production and decay. We therefore impose the following cuts on the final state partons (the subscript j refers to the extra jet only):⁴

$$\begin{aligned} |\eta_j|, |\eta_b| &\leq 2.5, \\ E_{Tj}, E_{Tb} &\geq E_T^{\min} = 10 \text{ GeV}. \end{aligned} \quad (2)$$

In addition, since the extra gluon jet must be distinguishable from the b jets, we require the gluon to be separated (in (η, ϕ) space) from the b and \bar{b} :

$$\Delta R_{bj}, \Delta R_{b\bar{b}} \geq 0.4. \quad (3)$$

The values of the cut parameters are deliberately chosen to mimic those in the actual experiments. They also serve to protect the theoretical cross section from the soft and collinear singularities of the matrix element. Other parameters are: $\sqrt{s} = 1.8 \text{ TeV}$, $m_t = 174 \text{ GeV}$, $\Gamma_t = 1.53 \text{ GeV}$, $m_b = 5.0 \text{ GeV}$, and $M_W = 80.0 \text{ GeV}$. We use MRS(A) parton distributions [11] with $\Lambda_{\overline{\text{MS}}}^{(4)} = 230 \text{ MeV}$, $\mu = m_t$ so that $\alpha_s = 0.103$.

With the above cuts, we obtain the total jet cross section

$$\sigma(p\bar{p} \rightarrow bW^+\bar{b}W^- + \text{jet} + X) = 2.0 \text{ pb}, \quad (4)$$

with 51% and 49% coming from the production and decay contributions respectively.⁵ This is to be compared to the leading-order cross section

$$\sigma(p\bar{p} \rightarrow bW^+\bar{b}W^- + X) = 3.8 \text{ pb}. \quad (5)$$

We note that the sum of these is not too far from the exact next-to-leading order total cross section of 4.9 pb calculated in Ref. [11]. Although it gives an indication of consistency in the calculations, this equivalence should not be taken too seriously. The cross sections in Eqs. (4) and (5) depend on the cuts applied to the final-state particles, and we have not included virtual gluon corrections to the lowest-order cross section. Furthermore, the $O(\alpha_s^3)$ cross section we calculate here contains what we might otherwise think of as corrections to two separate processes. Roughly speaking, part of the cross section in Eq. (4) is part of the $O(\alpha_s)$ correction to the $\Gamma(t \rightarrow bW)$ decay width, while the remainder is part of the $O(\alpha_s)$ ‘K-factor’ correction to the production cross section. In the limit $\Gamma_t \rightarrow 0$ this correspondence can be made exact – a full discussion can be found in Sec. 2.3 of Ref. [5].

⁴The cuts are applied to both the b and \bar{b} quarks.

⁵These percentages depend quite sensitively on the chosen cuts.

3.2 Jet distributions

In this section we study the distribution in phase space of the extra gluon jet, for the production, decay and total emission contributions, as was done in the soft-gluon analysis of Ref. [3]. We note that the cuts we use are slightly different from those used in Ref. [3], and this largely accounts for the differences in shapes of some of the distributions.

Fig. 2 shows the jet E_{Tj} distribution. The production (dot-dashed histogram) and decay (dotted histogram) contributions are broadly similar in shape, with a slight tendency for decay gluons to have higher E_T . Also shown, for comparison, is the E_T distribution of the b and \bar{b} quarks. As one would expect, the latter is significantly harder. More interesting is the jet pseudorapidity distribution shown in Fig. 3. Here we see a clear difference between the production and decay distributions. The former is broad, reflecting the importance of initial state radiation, while the latter is peaked in the central region, reflecting the tendency of the decay gluons to follow the directions of the b and \bar{b} quarks. The distribution is quite sensitive to the ΔR_{bj} separation cut. Decreasing this from its nominal value of 0.4 has little effect on the production part, but increases the decay part. This can be inferred from Fig. 4, where the distribution in the jet- b separation itself is shown. For production gluons, the dominance of initial-state radiation gives a broad distribution peaked at $\Delta R_{bj} \sim \pi/2$. For decay gluons, the collinear quasi-singularity when the gluons are emitted close to the b quarks (it is not a true singularity because the b 's are massive) gives rise to a sharp peak at small ΔR_{bj} . This figure illustrates the strong dependence of the relative proportions of production and decay contributions on the separation cut.

3.3 Invariant mass distributions

There are obvious problems in constructing the top mass from its decay products when there are additional jets in the final state. For example, the definition $m_t^2 = (p_b + p_W)^2$ will give the correct mass when the extra jet is a production gluon, but will *underestimate* the mass when it is a decay gluon. Conversely, the definition $m_t^2 = (p_b + p_W + p_j)^2$ will be correct for decay gluons, but will *overestimate* the mass for production gluons. Of course, this takes no account of the fact that any gross mismeasurement will be apparent when one compares the reconstructed masses of the t and \bar{t} . In principle, one can simply ignore permutations of the decay products which lead to $m_t \neq m_{\bar{t}}$.

In practice, however, given the experimental uncertainties in measuring the jet energies and in reconstructing one of the W bosons from its leptonic decay products, there is a danger of biasing the m_t measurement in events with extra jets, for example by adopting a strategy of not including such jets in the top quark four-momentum. For this reason, it is interesting to study the distortion of the top resonance in the

presence of extra jets.

Figure 5 shows the distribution in $m(bW)$, where $m(bW)^2 = (p_b + p_W)^2$. There are two entries for each event, corresponding to combining (say) the W^+ with both the b and the \bar{b} . The dashed histogram (production emission contribution) simply illustrates the smearing of the resonance peak from choosing the ‘wrong’ bW combination. The dotted histogram (decay emission contribution) has a significant shoulder on the lower side of the peak, showing the effect of omitting a gluon which was part of the top decay. The slight dip in the distribution below the peak reflects the E_T cut on the gluon jet. The net effect (solid histogram) is a distribution with a strong peak at m_t which is sitting on an asymmetric background, with a preference for lower mass values as expected. For purposes of comparison, the insert in Fig. 5 shows the leading order ‘correct combination’ $m_t \simeq m(bW)$ Breit-Wigner distribution with width $\Gamma_t = 1.53$ GeV.

When the extra jet is included in the mass reconstruction, the tendency is to overestimate the true mass. This is illustrated in Fig. 6, which shows the distribution in $m(bWj)$, where now $m(bWj)^2 = (p_b + p_W + p_j)^2$. In this case it is the production gluon emissions which generate a shoulder above the peak. There is also a similar effect from decay gluons which are emitted off the ‘wrong’ top quark.

An interesting feature of Figs. 5 and 6 is the much stronger broadening effect in the latter, in which there is a much larger contribution to the cross section *outside* the main peak. This is a consequence of the fact that there is a single extra jet in each event and can be understood as follows. Let us ignore wrong Wb pairings and consider only correct ones; the wrong pairings merely contribute smooth backgrounds to both figures. In each event at least one of the Wb pairs will reconstruct to m_t (up to finite-width and interference effects which we can ignore). Roughly half of these events will correspond to production emission, in which case the other Wb pair will also reconstruct to m_t . Hence 3/4 of correct Wb pairs contribute to the m_t peak in Fig. 5. Those same three-quarters of Wb pairs, when combined with the extra gluon jet, will then typically fall above the m_t peak in Fig. 6. The remaining one quarter, which fell below the peak in Fig. 5, *do* contribute to the m_t peak when combined with the extra jet, as in Fig. 6.

Figs. 5 and 6 show, then, that in events with extra jets, one cannot unambiguously reconstruct the top mass either by systematically excluding or including the jet momentum in the reconstruction. As suggested in Ref. [3], however, one might hope to utilize the different characteristics of production and decay emissions (as illustrated in Figs. 2–4) to devise a strategy for deciding whether to include the extra jets in the reconstruction. For example, since forward jets tend to be mostly from production (Fig. 3), one could decide to omit forward jets from mass reconstructions. In the central region, where both production and decay jets contribute significantly, one might gain by making assignments using weighting criteria according to, for example,

proximity to the b quarks. In any such procedure, of course, proper account must be taken of hadronization and detector resolution effects, which are beyond the scope of the present study.

3.4 Forward–backward asymmetry and color structure

Soft gluons are able to probe the color structure of a hard scattering process [4]. In Ref. [3] the distribution of the soft gluon jet was shown to be sensitive to the color structure of the process $q\bar{q} \rightarrow t\bar{t} \rightarrow b\bar{b}W^+W^-$ [12] (see also [4]). In particular, the \widehat{qt} antenna (or ‘string’) produces more radiation in the region between the t and q than, say, between the t and \bar{q} . In practice, the effect can be observed by comparing the probability of gluon radiation between the proton and the b quark with that between the proton and \bar{b} quark [3]. We are interested here in whether the asymmetry observed in Ref. [3] in the soft gluon approximation survives the more exact calculation of the present study.⁶

Following the same procedure as in Ref. [3] (but with the basic cuts given in Eqs. (2) and (3)), we define a subsample of $b\bar{b}W^+W^-$ + jet events in which the b and \bar{b} are separated by at least 135° in azimuth. This tends to select events in which the parent t and \bar{t} have similar separation. We then preferentially select gluon jets associated with the t (as opposed to the \bar{t}) by requiring that they lie within 90° in azimuth from the b quark. The η_g distribution of such jets should then be asymmetric, with more jets produced at forward rapidities, *i.e.*, between the directions of the b and the incoming p . Figure 7(a) shows that there is indeed a small forward–backward asymmetry. But note that this asymmetry is a feature of ‘production’ emission only – the ‘decay’ emission gives a symmetric pseudorapidity distribution (at least in the limit when $E_g \gg \Gamma_t$ so that interference contributions can be neglected). One can therefore enhance the asymmetry by increasing the separation cut ΔR_{bj} , thereby reducing the decay emission contribution. Figure 7(b) shows the corresponding η_g distribution when the cut is increased to $\Delta R_{bj} = 1.0$. It should also be possible to optimize the azimuthal angle cuts to enhance the effect.

4 Comparison with HERWIG

We have already seen that the cross section for the emission of an extra jet in $t\bar{t}$ production has a very rich structure, with the two main contributions coming from production and decay emission. We have given examples of how this relates to simple top mass reconstruction scenarios. It is vitally important that the programs used in the actual experimental analyses, which must of course take hadronization and

⁶Note that the extra gg and qg processes included here but omitted in Ref. [3] tend to dilute the asymmetry.

detector effects fully into account and are therefore much more sophisticated than our parton-level calculations, contain as much of this structure as possible.

It is not our intention here to make an exhaustive comparison with all the available programs for simulating top production. Instead, we compare our predictions for the jet distributions with those of the HERWIG Monte Carlo program (v5.8) [10], which is widely used in collider physics. This comparison is not at all straightforward, even when hadronization is switched off, since the Monte Carlo program can generate $t\bar{t}$ events with many additional quarks and gluons in the final state. We must therefore introduce a simple jet algorithm for clustering these partons. Specifically, we draw cones in $\eta - \phi$ space around the b quarks and around any additional energetic partons in the final state, and assign all transverse energy within the cones to the jet. In this way we obtain a final state with b -jets (which contain a b quark and possibly other partons) and additional jets originating in energetic, wide-angle quark and gluon bremsstrahlung. The default cone size for clustering is chosen to be $\Delta R = 0.4$. We then apply the cuts of Eqs. (2) and (3) and select those events with one and only one additional jet,⁷ and compare this $b\bar{b}W^+W^- + \text{jet}$ sample (labeled PS for ‘parton shower’ in the figures below) with that generated by our tree-level matrix element calculation (labeled ME).

Fig. 8 shows the normalized distributions in (a) the jet- b separation ΔR_{bj} , (b) the jet pseudorapidity η_j , (c) the jet E_T , and (d) the jet energy E_j in the parton subprocess center-of-mass frame. The first two show significant differences in shape. It would appear that the PS calculation produces *too few jets in the direction of the b quarks*. In fact one can see in the PS distribution in Fig. 8(a) a clear separation between the ‘production’ jets, which are widely separated from the b quarks in general, and the ‘decay’ jets which prefer to be close to the b quarks. The ME calculation evidently produces more of the latter and the dip is filled in. The same effect is seen in the η_j distribution, Fig. 8(b). The peaking at $\eta_j = 0$ in our ME calculation is caused by a sizeable contribution from ‘decay’ gluons produced close to the centrally-produced b quarks. Interestingly, the energy distributions shown in Fig. 8(c) are very similar. However, the preference for more centrally produced jets in the ME calculation produces a harder jet E_T spectrum, Fig. 8(d).

Fig. 9 shows the $m(bW)$ and $m(bWj)$ distributions for the ME and PS calculations.⁸ The differences simply reflect the different behaviours already seen in Fig. 8. There are more PS events in the peak at m_t in the $m(bW)$ distribution, and consequently fewer peak events in the $m(bWj)$ distribution, since the PS calculation has apparently fewer jets emitted in the decay process.

As noted above, the PS calculation requires a jet algorithm to cluster partons into jets. We have tried varying the cone size away from its nominal value of 0.4 to see if we

⁷With the jet definition used here, most events with jets contain only one.

⁸For purposes of comparison we include only the ‘correct’ bW^+ and $\bar{b}W^-$ combinations in Fig. 9.

can improve the agreement between the ME and PS results. We find, however, that the changes that result are small in comparison with the discrepancy (in particular for the ΔR_{bj} distribution) between the models.

We have no simple explanation as to why the PS calculation appears to give qualitatively different distributions in jet variables than our exact calculation, except to note that the differences appear to originate in the relative number of jets produced in top production and decay. Traditionally, ME and PS calculations are expected to agree quite well, except when the final state contains very energetic, widely-spaced parton jets; see for example the study in Ref. [13] for $W + \text{jets}$ production. For such configurations, the leading-logarithm approximation inherent in the PS approach is expected to break down. However, we note that our cuts as defined in Eqs. (2) and (3) are not very stringent, and therefore *not* particularly biased in favor of such events. In fact, we have checked that the ΔR_{bj} calculated using the soft-gluon approximation of Ref. [3] is very similar to the result of the exact (ME) calculation shown in Fig. 8.

5 Conclusions

It is important that experimental data analyses are based on predictions that account for all relevant physical effects. In the case of the top quark, one very relevant physical effect is the presence of extra jets in top events. We have presented the results of the first exact calculation of hadronic $t\bar{t}$ production and decay in association with an additional jet, taking into account all Feynman diagrams that can contribute, including both resonant and non-resonant top production and all interferences. This extends the work of Ref. [3] to gluons of arbitrary energies, and allows for a more complete and exact analysis.

We have studied the distribution of such extra jets, and showed that the cross section can be decomposed into emissions associated with top production and with top decay, according to a gauge-invariant operational definition. This decomposition is particularly relevant to top mass reconstruction, and our motivation was, in part, to consider the consequences for top mass measurement of the presence of such extra jets in top events. We have seen that extra jets can give rise to shoulders outside the Breit-Wigner peak in Wb and $Wb + \text{jet}$ invariant mass distributions, potentially degrading the resolution for top mass measurements.

We have also considered distributions generated with the HERWIG parton-shower Monte Carlo program, which is a major analysis tool for the experiments and which uses a collinear approximation to simulate emission of gluons. After defining a jet clustering algorithm that allowed us to compare our matrix element results with those of HERWIG, we have found some discrepancies. These appear to indicate a relatively smaller contribution from decay gluons generated by HERWIG, but we are unable to explain the difference in detail.

Acknowledgements

Two of us (TS,WJS) are grateful to the UK PPARC for a Post-Doctoral and Senior Fellowship respectively. Useful discussions with Valery Khoze, Michelangelo Mangano, and Bryan Webber are acknowledged. This work was supported in part by the U.S. Department of Energy, under grant DE-FG02-91ER40685 and by the EU Programme “Human Capital and Mobility”, Network “Physics at High Energy Colliders”, contract CHRX-CT93-0537 (DG 12 COMA).

References

- [1] CDF collaboration: F. Abe *et al.*, Phys. Rev. **D50** (1994) 2966; Phys. Rev. Lett. **73** (1994) 225.
- [2] D0 collaboration: S. Abachi *et al.*, Phys. Rev. Lett. **72** (1994) 2138; Fermilab preprint November 1994.
- [3] L.H. Orr and W.J. Stirling, Durham University preprint DTP/94/60 (1994), hep-ph/9409238, to be published in Phys. Rev. **D**.
- [4] Yu.L. Dokshitzer, V.A. Khoze, A.H. Mueller, and S.I. Troyan, *Basics of Perturbative QCD*, Editions Frontieres, 1991.
- [5] V.A. Khoze, L.H. Orr and W.J. Stirling, Nucl. Phys. **B378** (1992) 413.
- [6] V.A. Khoze, J. Ohnemus and W.J. Stirling, Phys. Rev. **D49** (1994) 1237.
- [7] B. Lampe, preprint MPI-Ph/94-67 (1994).
- [8] F.A. Berends, W.T. Giele, H. Kuijf and B. Tausk, Nucl. Phys. **B357** (1991) 32.
- [9] T. Stelzer, W.F. Long, Comp. Phys. Commun. **81** (1994) 357.
- [10] G. Marchesini and B.R. Webber, Nucl. Phys. **B310** (1988) 461.
G. Marchesini, B.R. Webber, G. Abbiendi, I.G. Knowles, M.H. Seymour and L. Stanco, Comp. Phys. Commun. **67** (1992) 465.
- [11] A.D. Martin, R.G. Roberts and W.J. Stirling, University of Durham preprint DTP/94/34 (1994), to be published in Phys. Rev. **D**.
- [12] G. Marchesini and B.R. Webber, Nucl. Phys. **B330** (1990) 261.

- [13] W.T. Giele, T. Matsuura, M.H Seymour and B.R. Webber, Contribution to Proc. of 1990 Summer Study on High Energy Physics: Research Directions for the Decade, Snowmass, CO, June 25 - July 13, 1990.

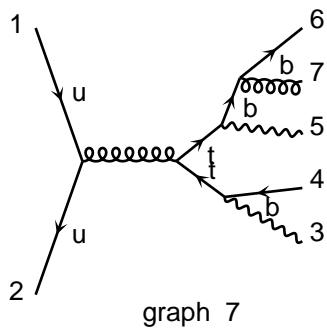
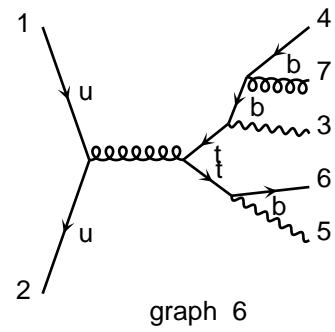
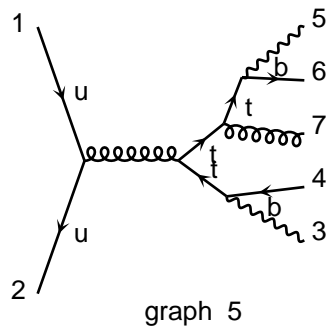
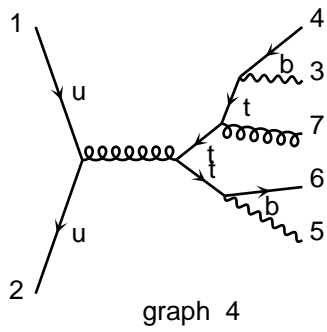
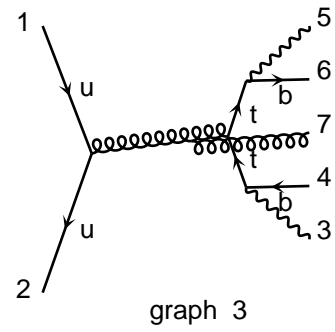
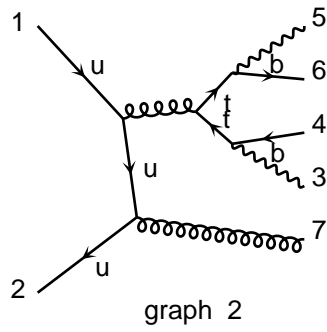
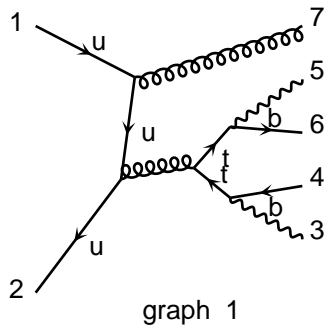
Figure Captions

- [1] The subset of (7) Feynman diagrams which dominate the cross section for the production of extra jets in top production.
- [2] The E_T distribution (solid histogram) of the extra jet produced in association with $t\bar{t}$ in $p\bar{p}$ collisions at $\sqrt{s} = 1.8$ TeV, together with its decomposition in terms of production (dot-dashed histogram) and decay (dotted histogram) emission contributions. Also shown is the E_T distribution of the b and \bar{b} quarks.
- [3] The extra jet pseudorapidity (η_j) distribution (solid histogram) and its decomposition in terms of production (dot-dashed histogram) and decay (dotted histogram) emission contributions.
- [4] The Lego-plot jet- b separation ($\Delta R_{bj} = (\Delta\eta_{bj}^2 + \Delta\phi_{bj}^2)^{1/2}$) distribution (solid histogram) and its decomposition in terms of production (dot-dashed histogram) and decay (dotted histogram) emission contributions.
- [5] The distribution (solid histogram) in the Wb invariant mass, $m(bW)^2 = (p_b + p_W)^2$. Also shown are the distributions corresponding to the production (dot-dashed histogram) and decay (dotted histogram) emission contributions.
- [6] The distribution (solid histogram) in the $Wb + \text{jet}$ invariant mass, $m(bWj)^2 = (p_b + p_W + p_j)^2$. Also shown are the distributions corresponding to the production (dot-dashed histogram) and decay (dotted histogram) emission contributions.
- [7] The jet pseudorapidity asymmetry distribution (solid histogram) defined in the text, and its decomposition in terms of production (dot-dashed histogram) and decay (dotted histogram) emission contributions, for (a) $\Delta R_{bj} > 0.4$ and (b) $\Delta R_{bj} > 1.0$.
- [8] Distributions in (a) the jet- b separation ΔR_{bj} , (b) the jet pseudorapidity η_j , (c) the jet E_T , and (d) the jet energy E_j in the subprocess center-of-mass frame, for the exact calculation (solid histograms, labeled ME) and as obtained using the HERWIG parton-shower Monte Carlo program (dashed histograms, labeled PS).
- [9] As in Fig. 8, but for the Wb and $Wb + \text{jet}$ invariant mass distributions.

This figure "fig1-1.png" is available in "png" format from:

<http://arxiv.org/ps/hep-ph/9412294v1>

Diagrams by MadGraph



This figure "fig2-1.png" is available in "png" format from:

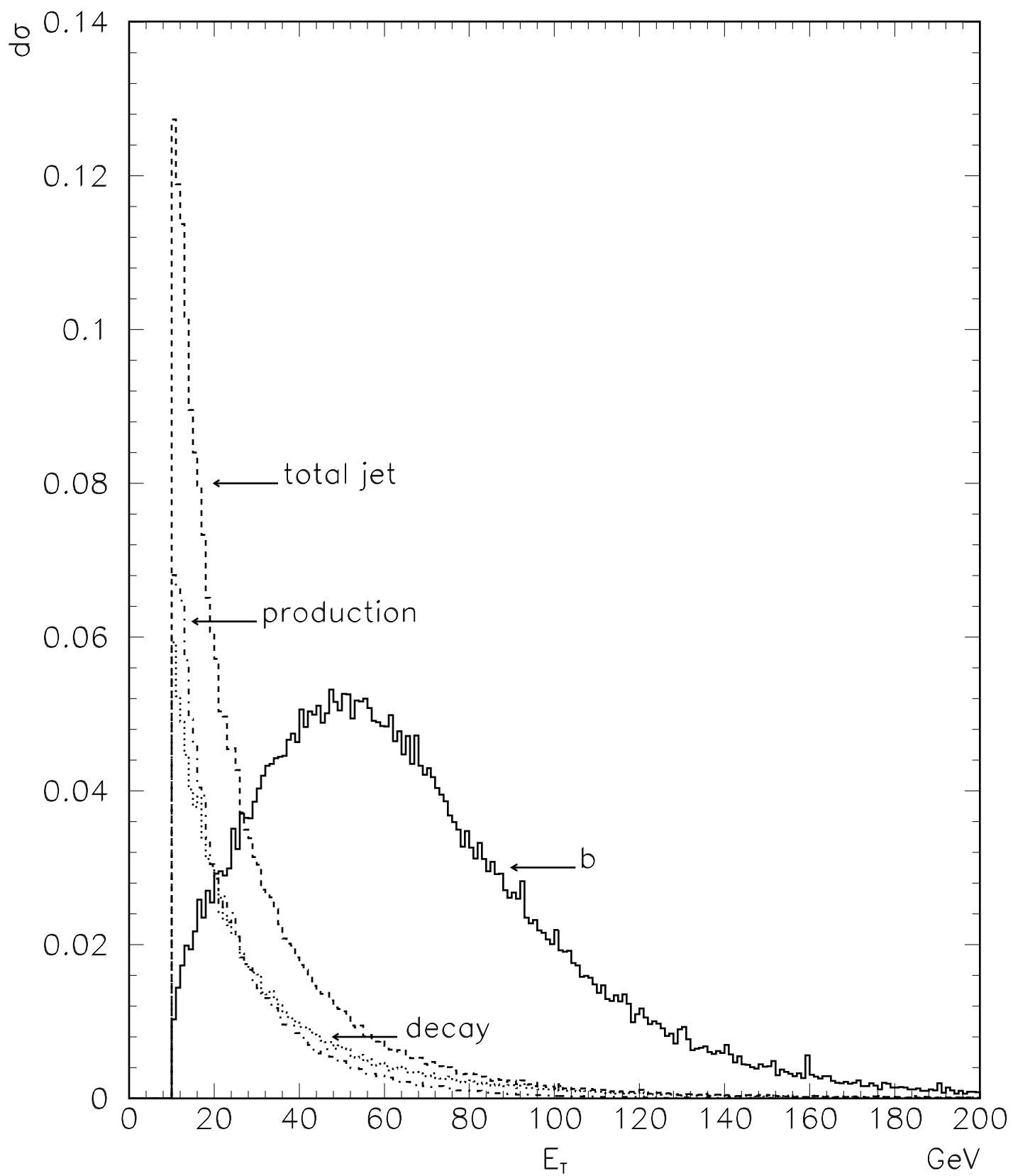
<http://arxiv.org/ps/hep-ph/9412294v1>

This figure "fig1-2.png" is available in "png" format from:

<http://arxiv.org/ps/hep-ph/9412294v1>

This figure "fig2-2.png" is available in "png" format from:

<http://arxiv.org/ps/hep-ph/9412294v1>

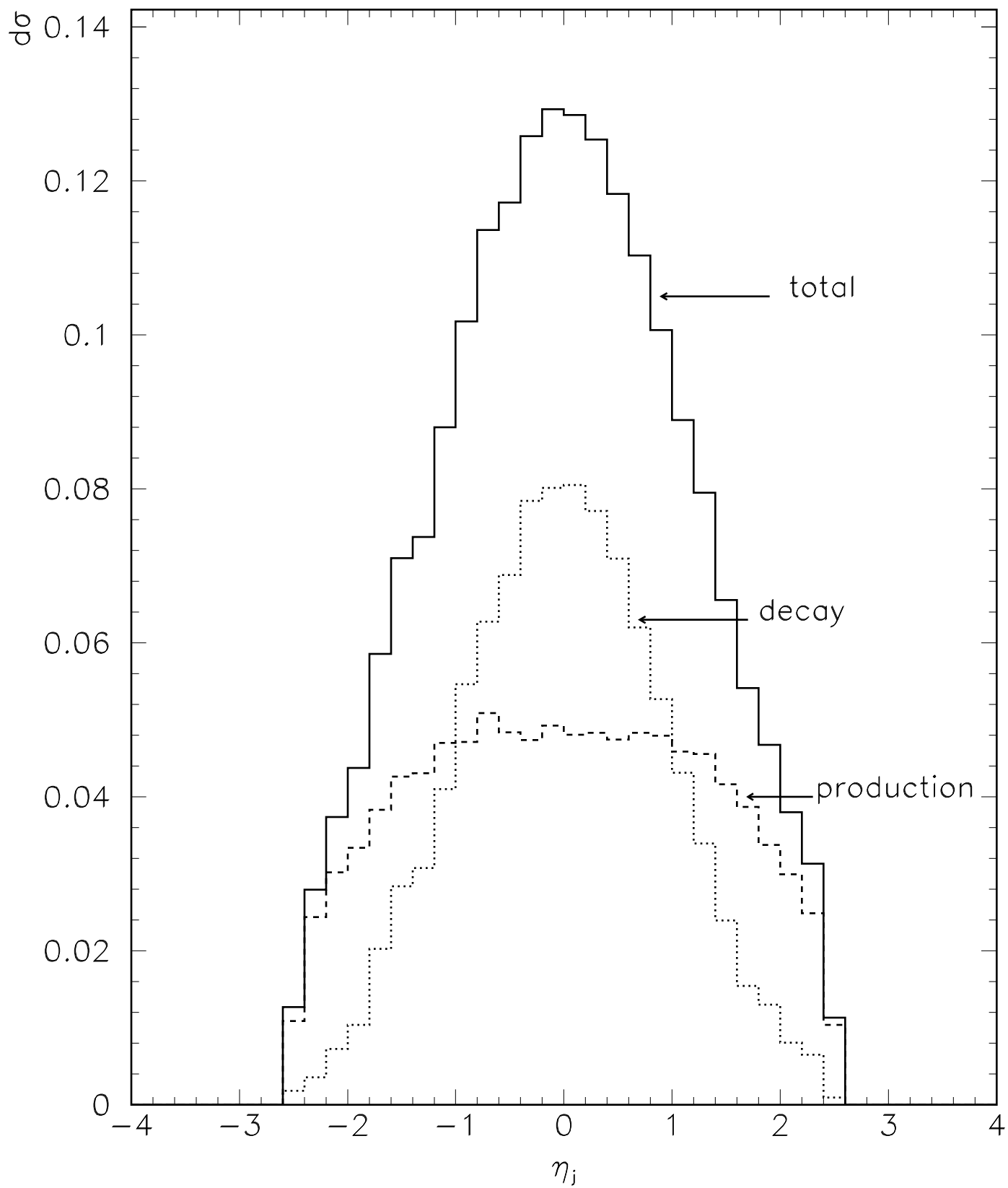


This figure "fig1-3.png" is available in "png" format from:

<http://arxiv.org/ps/hep-ph/9412294v1>

This figure "fig2-3.png" is available in "png" format from:

<http://arxiv.org/ps/hep-ph/9412294v1>

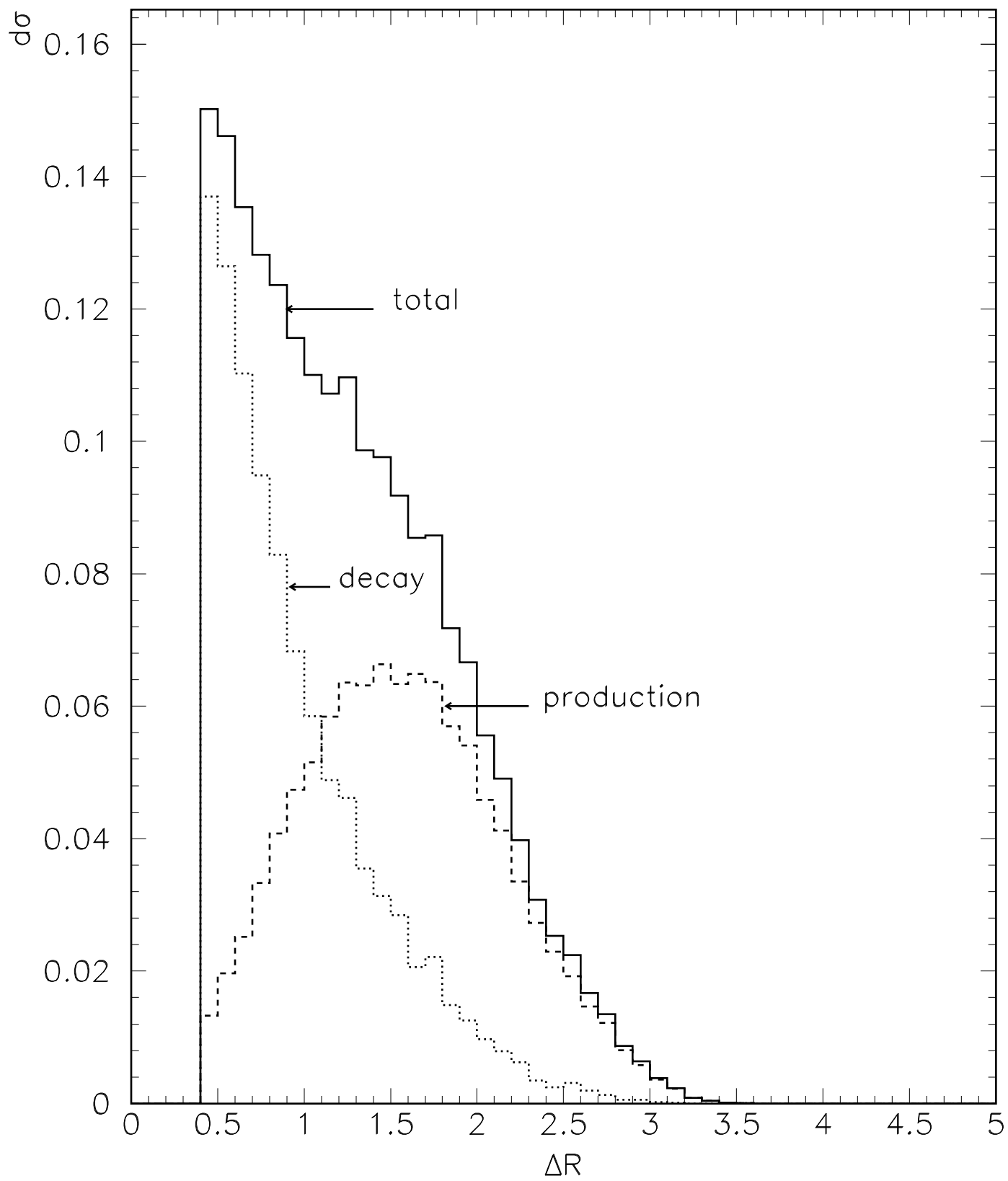


This figure "fig1-4.png" is available in "png" format from:

<http://arxiv.org/ps/hep-ph/9412294v1>

This figure "fig2-4.png" is available in "png" format from:

<http://arxiv.org/ps/hep-ph/9412294v1>



This figure "fig1-5.png" is available in "png" format from:

<http://arxiv.org/ps/hep-ph/9412294v1>

